Inorganic Chemistry

Article

pubs.acs.org/IC

Clarifying the Mechanism of Cation Exchange in Ca(II)[15-MC$_{Cu(II)Ligand}$-5] Complexes

Choong-Sun Lim,[†] Matteo Tegoni,[‡] Tamás Jakusch,[†] Jeff W. Kampf,[†] and Vincent L. Pecoraro*[,†]

[†]Department of Chemistry, University of Michigan, Ann Arbor, Michigan 48109-1055, United States

[‡]Department of Chemistry, University of Parma, Parma 43124, Italy

Supporting Information

ABSTRACT: The calcium metallacrown Ca(II)[15-MC$_{Cu(II)N(Trpha)}$-5]$^{2+}$ was obtained by self-assembly of Ca^{II}, Cu^{II}, and tryptophanhydroxamic acid. Its X-ray structure shows that the core calcium ion is well-encapsulated in the five oxygen cavity of the metallacrown scaffold. The kinetics of Ca−Ln core metal substitution was studied by visible spectrophotometry by addition of Ln^{III} nitrate to solutions of Ca(II)[15-MC$_{Cu(II)N(Trpha)}$-5]$^{2+}$ in methanol solution at pH 6.2 (Ln^{III} = La^{III}, Nd^{III}, Gd^{III}, Dy^{III}, Er^{III}) to obtain the corresponding Ln(III)[15-MC$_{Cu(II)N(Trpha)}$-5]$^{3+}$ complexes on the hours time scale. The reaction is first order in the two reactants (second order overall) with different rate constants across the lanthanide series. In particular, the rate for the Ca−Ln substitution decreases from La^{III} to Gd^{III} and then increases slightly from Gd^{III} to Er^{III}. This substitution reaction occurs with second order rate constants ranging from 0.1543(3) M^{-1} min^{-1} for La^{III} to 0.0720(6) M^{-1} min^{-1} for Gd^{III}. By means of the thermodynamic log *K* constants for the same reaction previously reported, the rate constants for the inverse Ln−Ca substitution were also determined. In this study, we demonstrated that the substitution reaction proceeds through a direct metal substitution and does not involve the disassembly of the MC scaffold. These observations in concert allow the proposition of a hypothesis that the dimension of the core metals play the major role in determining the rate constants of the substitution reaction. In particular, the largest lanthanides, which do not require complete encapsulation in the MC cavity, displace the Ca^{II} ion faster, whereas in the back reaction Ca^{II} displaces the smaller lanthanides faster as they interact relatively weakly with the metallacrown oxygen cavity.

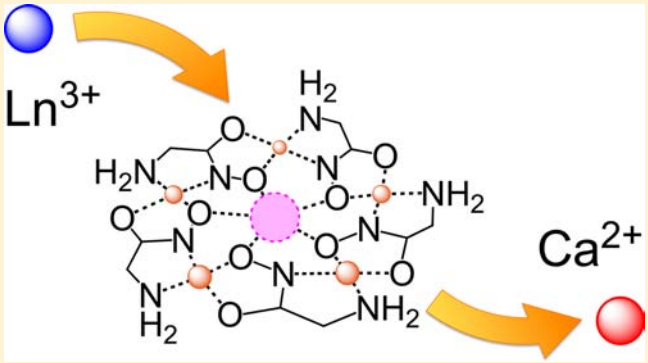

INTRODUCTION

Metallacrowns are the inorganic analogues of crown ethers,[1−3] and since their recognition in 1989,[4,5] they have been studied for their interesting capabilities as hosts for cations and anions. Metallacrowns generally have been shown to sequester ions including Li^{I},[6] Na^{I},[6−9] K^{I},[6,8] Mn^{II},[10] Cu^{II},[10−17] and Ni^{II},[18,19] as 12-MC-4 structures. Although 15-MC-5 complexes with salicylhydroxamic acid could be prepared solely as mixed valence manganese complexes,[20] the copper 15-metallacrowns-5 complexes of α-aminohydroxamic acids (Scheme 1) were shown to be able to encapsulate a number of metal ions such as Y^{III},[21−23] Na^{I},[23] Ag^{I},[23] Pb^{II},[23] Hg^{II},[23] Ca^{II},[24,25] Ln^{III},[1−3,26−29] and UO$_2^{VI}$.[30−32] For the last three core cations it was established that the order of stability of the corresponding 15-MC-5 is Ca^{II} < Ln^{III} < UO$_2^{VI}$.[24,30−32] As regards the Ln(III)[15-MC$_{Cu(II)N(L)}$-5]$^{3+}$ complexes (L = Pheha, Trpha, Scheme 1), we have recently determined their relative stability for different lanthanides in methanolic solutions through the study of the Ca−Ln substitutition reactions.[24] These investigations showed that the 15-MC-5 with lighter, larger lanthanides are more stable than those with smaller, heavier ones. More important, those studies showed that for lighter lanthanides (Ln-Gd) the stability of the Ln(III)[15-MC$_{Cu(II)N(L)}$-5]$^{3+}$ complexes is very similar, while there is a significant decrease in the log *K* of

Scheme 1. Schematic Representation of a 15-MC-5 Complex of Trpha (R = R$_1$) and Pheha (R = R$_2$)[a]

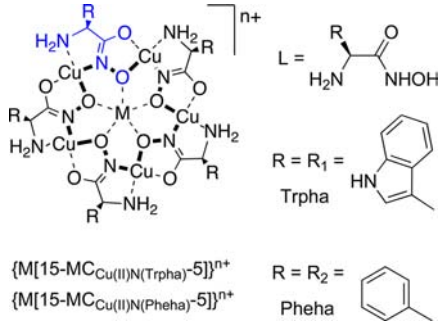

[a]In this work, M = Ca^{II}, La^{III}, Nd^{III}, Gd^{III}, Dy^{III}, Er^{III}. One deprotonated ligand in the assembled metallacrown is depicted in blue.

Received: June 27, 2012
Published: October 17, 2012

formation in the case of heavier lanthanides.[24] The thermodynamic selectivity in the formation of these complexes by substitution of the core Ca^{II} ion was explained by taking into account the different dimension of the Ln^{III} ions, their capability to interact with the MC cavity and their desolvation energies.[24]

Recently, the effect of the dimension of the central lanthanide ion in Ln(III)[15-$MC_{Cu(II)N(Pheha)}$-5]$^{3+}$ complexes in the solid state has been examined,[29] leading to the conclusion that the fine structural features (planarity, cavity dimension etc.) and likely the complexation capabilities of the 15-MC-5 scaffold arise from a delicate balance of several factors, among which the nature and dimension of the central lanthanide are of paramount importance. In this paper, we present the first kinetic investigation of central cation substitution by examining Ca−Ln substitution for the metallacrown Ca(II)[15-$MC_{Cu(II)N(Trpha)}$-5]$^{2+}$ (**1**) with different lanthanide(III) ions (La^{III}, Nd^{III}, Gd^{III}, Dy^{III}, Er^{III}). The kinetics for this reaction was studied by visible spectroscopy, and the rate constants were correlated with the thermodynamic parameter (log *K*) for the same reaction reported previously.[24] The aim of these studies is to understand more completely at a molecular level the complexation of cations by metallacrowns and to define a possible correlation between the kinetics of core metal substitution in 15-MC-5 complexes with the dimension of the lanthanide ions. These data can be used together with the thermodynamic behavior[3,24] and the structural features[2,29] in the solid state to devise new 15-MC-5 based materials for the selective encapsulation of lanthanides.

EXPERIMENTAL SECTION

Materials. Lanthanide nitrates, copper acetate, calcium nitrate, MES buffer, L-tryptophan-, and L-phenylalanine methyl ester hydrochloride were obtained from Sigma-Aldrich. Methanol was received from Fisher Scientific and used without purification. L-Tryptophanhydroxamic acid and L-phenylalaninehydroxamic acid were synthesized as previously reported in the literature.[24] The purity of the ligands was checked by NMR and elemental analysis. ^{1}H NMR spectra were collected on a Varian Inova 400 MHz or Bruker Avance 300 MHz spectrometers. Elemental analyses (CHN) were carried out by a Carlo Erba EA1108 microanalyzer.

Synthesis of {Ca(II)[15-$MC_{Cu(II)N(Trpha)}$-5]}$(NO_3)_{1.5}(CH_3O)_{0.5}$ (1). This complex has been synthesized following the reported procedure,[24] as follows: L-tryptophanhydroxamic acid (0.10 g, 0.55 mmol) and copper acetate dihydrate (0.11 g, 0.56 mmol) were dissolved in 50 mL of methanol and stirred for 10 min. Calcium nitrate tetrahydrate (0.026 g, 0.11 mmol) was added to green solution and the color changed to brick red. The solution was stirred overnight and the green insoluble impurities were filtered out. By slow evaporation, a brown powder precipitated out. The product was filtered out and recrystallized in a methanol/water mixture (99:1) to obtain brown red crystals. The crystal was analyzed with X-ray diffraction method. Yield = 24%. ^{1}H NMR [CD_3OD, 300 MHz]: δ 29.5 (br, 5H, C_αH), 10.2 (br, 5H, C_βH), 9.5 (br, 5H, C_βH), 7.39 (br s, 10H, C_{indole}H), 7.07 (br, 10H, C_{indole}H). ESI-MS: *m*/*z* 722 ({Ca(II)[15-$MC_{Cu(II)N(Trpha)}$-5]}$^{2+}$), 1506 ({Ca(II)[15-$MC_{Cu(II)N(Trpha)}$-5]}$(NO_3)^+$). Anal. Calcd for $C_{56.5}H_{73}CaCu_5N_{16.5}O_{22.25}$: C, 39.99; H, 4.34; N, 13.62. Found: C, 40.1; H, 4.4, N, 13.8.

Synthesis of {Ca(II)[15-$MC_{Cu(II)N(Pheha)}$-5]}$(CH_3OH)(OH_2)_{7.5}(NO_3)_2$ (2). This complex has been synthesized following the reported procedure,[24] as follows: L-phenylalaninehydroxamic acid (0.123 g, 0.561 mmol), calcium nitrate tetrahydrate (0.026 g, 0.11 mmol), and copper acetate dihydrate (0.11 g, 0.56 mmol) were dissolved in 30 mL of methanol. The solution was stirred for 24 h. The solution was filtered to remove the green impurities and slowly evaporated to obtain a reddish brown microcrystalline powder of the complex. Yield 31%. ^{1}H NMR [CD_3OD, 300 MHz]: δ 24.7 (br, 5H, C_αH), 12.4 (br, 5H, C_βH), 7.9 (br, 5H, C_βH), 7.34 (br s, 15H, Ph), 7.05 (br s, 10H, Ph). ESI-MS: *m*/*z* 1504 ({Ca(II)[15-$MC_{Cu(II)N(Pheha)}$-5]}$(NO_3)^+$). Anal. Calcd for $C_{46}H_{69}CaCu_5N_{12}O_{24.5}$: C, 35.88; H, 4.52; N, 10.91. Found: C, 35.7; H, 4.2, N, 10.8.

Spectrophotometric Measurements and Calculations. Visible absorption spectra were collected on a Varian Cary 100 Bio spectrophotometer using matched quartz cells of 1 cm of path length. Temperature was kept constant to 293.16 K during all the measurements, using an external thermostatting bath connected to the cuvette holder. A stock solution of **1** (5 mM) was prepared by weight in 50 mM MES buffer in methanol (pH 6.2). The samples for the study of the order of reaction were prepared with fixed **1** concentration (2.1 mM) and C_{Gd} = 10−30 mM, or at fixed Gd^{III} concentration (90 mM) and C_1 = 0.39−1.91 mM. A table with the concentrations used for this experiment is given as a Supporting Information. Samples of **1** (C_1 = 0.39 to 2.10 mM) were obtained by dilution of the concentrated stock solution with buffer solution directly in the cuvette, to obtain 3 mL samples. To start the reaction, solid Gd^{III} nitrate (13.6 to 122 mg) was added to the solutions in the cuvette to obtain a C_{Gd} = 10−90 mM, and the spectra registered every 30 min for 20 h, and then every 6−12 h for 4 days. The reaction rate was calculated as the variation of the concentration of **1** as a function of time ($[\mathbf{1}]_t$), using the formula $[\mathbf{1}]_t = [\mathbf{1}]_0(A_t^{490\ nm} - A_\infty^{490\ nm})/(A_0^{490\ nm} - A_\infty^{490\ nm})$ where $[\mathbf{1}]_0$ is the initial concentration of **1**, and A_t, A_0 and A_∞ are the absorbance values at 490 nm at given time, initial and at infinite time, respectively. The initial rates of reaction were determined using the $[\mathbf{1}]_t$ values at *t* = 0, 30, 60, and 90 min where they resulted in the linear regime. The calculation of the reaction rates was performed by the SPSS 20 program.[33] The determination of the rate constants for the Ca−Ln substitution reaction was performed as follows. Samples containing **1** at a 1.85 mM concentration were obtained by dilution of the concentrated stock solution with buffer solution directly into the cuvette, to obtain 3 mL samples. Solid Ln^{III} nitrate (ca. 25 mg) was added to the solution in the cuvette to obtain a C_{Ln} = 18.5 mM, and the spectra registered every 30 min for 20 h, and then every 6−12 h for 4−6 days. A second-order kinetic model was used to treat the spectra in the 430−750 nm range up to 20 h after reactants mixing. The calculation of the second order rate constants for the Ca−Ln substitution reaction were performed treating the visible spectra in the range 450−700 nm with the SPECFIT 32 program.[34] The calculation of the activation energies has been performed using the Eyring equation (see the Supporting Information), assuming a transmission coefficient equal to unity.

ESI-MS Studies. ESI mass spectra were recorded on a single quadrupole ZMD Mass Spectrometer (Micromass, Manchester, UK) fitted with a pneumatically assisted electrospray probe. Data were processed using the spectrometer software (MassLynx NT version 3.4). The measurements were performed on three solutions prepared as follows. A 2.22 × 10^{-2} M solution of La^{III} was prepared dissolving 96.1 mg (0.222 mmol) of lanthanum(III) nitrate hexahydrate in 10 mL of methanol. Two solutions containing **1** or **2** (ca. 1.7−1.8 × 10^{-3} M) were prepared by weight dissolving the solid compounds in 5 mL of methanol (**1**: 14.5 mg, 8.57 mmol; **2**: 15.1 mg, 8.86 mmol). Two aliquots of 1.5 mL of the two solutions were mixed to obtain two samples (3 mL) containing equimolar concentrations of **1** and **2** (final $C_1 = C_2$ = 8.9 × 10^{-4} M). One of the samples was added with 0.5 mL of the La^{III} solution (0.0111 mmol) obtaining a solution containing a La^{III}/Ca^{II} = 2.1:1 ratio. The two samples (in the presence and absence of La^{III}) were analyzed by ESI-MS after 72 h. A control solution was prepared by dissolving lanthanum(III) nitrate pentahydrate (6.3 mg, 0.015 mmol), copper acetate monohydrate (9.0 mg, 0.045 mmol), Trpha (11.3 mg, 0.052 mmol) and Pheha (8.6 mg, 0.048 mmol) in 10 mL of methanol. The solution was left to equilibrate for 72 h and analyzed by ESI-MS. The solutions were analyzed by infusion through an HPLC pump in positive ion mode using a 10 μL sample loop and a 10 mL/min flux of methanol as eluent. The conditions were: ES capillary 3.0 kV; cone 60−120 V; extractor 4 V, source block temperature 80 °C, desolvation temperature 150 °C.

X-ray Crystal Determination. Brown red blocks of **1** were crystallized from a water/methanol solution at 23 °C. A crystal of dimensions 0.23 × 0.23 × 0.16 mm^3 was mounted on a standard Bruker SMART APEX CCD-based X-ray diffractometer equipped with a low-temperature device and fine-focus Mo-target X-ray tube (λ = 0.71073 Å) operated at 1500 W power (50 kV, 30 mA). The X-ray intensities were measured at 85(2) K; the detector was placed at a distance 5.055 cm from the crystal. A total of 2420 frames were collected with a scan width of 0.5° in ω and 0.45° in Φ with an exposure time of 60 s/frame. Indexing was performed by use of the CELL_NOW program[35] which indicated that the crystal was a two-component, nonmerohedral twin. The frames were integrated with the Bruker SAINT software package with a narrow frame algorithm.[36] The integration of the data yielded a total of 386 389 reflections to a maximum 2θ value of 45.44°, of which 21 378 were independent and 17 093 were greater than 2σ(I). The final cell constants (Table 1) were based on the xyz centroids of 9168 reflections above 10σ(I). Analysis of the data showed negligible decay during data collection; the data were processed with TWINABS and corrected for absorption.[37] The domains are related by a rotation of 179.7° about the reciprocal and direct [1 0 0] axis. For this refinement, single and composite reflections from the primary domain were used. Merging of the data was performed in TWINABS and an HKLF 4 format file used for refinement. The structure was solved and refined with the Bruker SHELXTL (version 2008/3) software package,[38] using the space group P2(1)2(1)2(1) with Z = 4 for the formula $C_{113}H_{146}N_{30}O_{44.5}Ca_2Cu_{10}$. All non-hydrogen atoms were refined anisotropically with the hydrogen atoms placed in idealized positions. Full-matrix least-squares refinement based on F^2 converged at R1 = 0.0692 and wR2 = 0.1923 [based on $I > 2\sigma(I)$], R1 = 0.0829 and wR2 = 0.2038 for all data. Additional details are presented in Table 1 and are given as Supporting Information in a CIF file.

Table 1. Crystallographic Data of {Ca(II)[15-MC$_{Cu(II)N(Trpha)}$-5]}$(NO_3)_{1.5}(CH_3O)_{0.5}$ (1)

	1
empirical formula	C_{113} H_{146} Ca_2 Cu_{10} N_{33} $O_{44.50}$
space group	$P2(1)2(1)2(1)$
cryst syst	orthorhombic
M	3394.19
a (Å)	17.3716(11)
b (Å)	23.8471(14)
c (Å)	38.716(2)
α (deg)	90.00
β (deg)	90.00
γ (deg)	90.00
V (Å^3)	16038.5(17)
Z	4
D_{calcd}	1.406
abs. coeff. (mm^{-1})	1.443
no. of reflns collected/unique	386389/21378
R(int)	0.0739
GOF	1.052
wR2[$I > 2\sigma(I)$]	0.1923
R1[$I > 2\sigma(I)$]	0.0692
wR2 (all data)	0.2038
R1 (all data)	0.0829

[a] $wR2 = |\sum w(|F_o|^2 - |F_c|^2)|/\sum|w(F_o)^2|^{1/2}$, $w = 1/[\sigma^2(F_o^2) + (mP)^2 + nP]$ and $P = [\max(F_o^2,0) + 2F_c^2)]/3$ (m and n are constants); $\sigma = [\sum[w(F_o^2 - F_c^2)^2]/(n - p)]^{1/2}$. [b] $R1 = \sum||F_o| - |F_c||/\sum|F_o|$.

RESULTS

Structural Description. The crystal structure of **1** (Figure 1), obtained from a methanol/water solution contains two metallacrowns in one unit cell. The structure is typical for copper(II) 15-MC-5 complexes with α-aminohydroxamic acids reported in the literature.[2,25,29,39] In both metallacrowns, the core calcium ion has a coordination number of 7, where five positions in the equatorial plane are occupied by the oxygens of the MC cavity and the two axial positions (above and below the cavity plane) are occupied by water molecules. In one of the two metallacrowns, all five copper ions are square pyramidal. For two of them, the fifth axial position is occupied by a water molecule, while two bind to the oxygen of a monodentate nitrate ion and the fifth copper coordinates a methoxide ion. The second metallacrown has three square planar copper ions, whereas the remaining two are square pyramidal with the fifth axial position occupied by either a water molecule or the oxygen of a third nitrate ion, which also provides for the fourth negative charge for charge balance. The core calcium ion is almost perfectly encapsulated into the MC cavity, with a maximum deviation from the oxygens mean plane of only 0.06 Å. Interestingly, the deviation from the oxygen mean plane is smaller for Ca^{II} than for Gd^{III} (8 coordinate) despite their similar ionic radii (1.06 and 1.057 Å, respectively).[29,40]

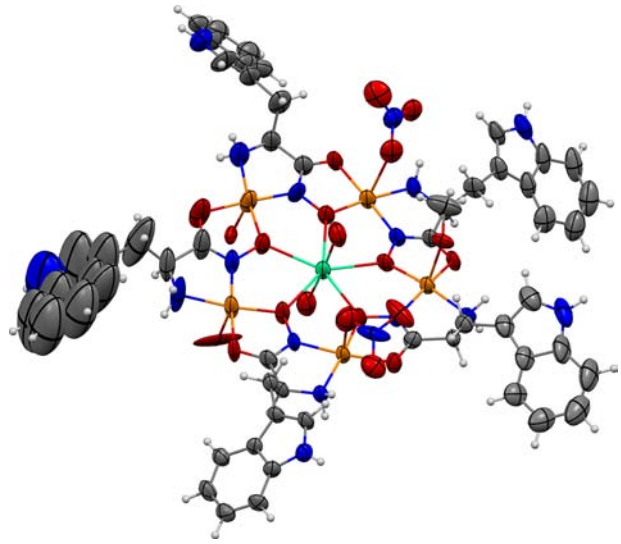

Figure 1. X-ray crystal structure of **1**, top view. Lattice solvent/anions have been omitted for clarity. Color scheme: gray = carbon; red = oxygen; blue = nitrogen; orange = Cu^{II}; green = Ca^{II}. Thermal ellipsoids displayed at 50% probability.

As already observed for several Ln^{III} MC complexes of phenylalaninehydroxamic acid with nitrate as counter-ion,[21,29,41−43] the side residues in this metallacrown do not point toward the center of the MC scaffold but they are oriented on the outside of the MC scaffold. As a consequence, no hydrophobic cavity is observed on one side of the MC plane, and the MC scaffolds orient in a parallel fashion in the crystal packing. The metallacrowns planes are connected through interactions that involve both the hydrophilic and the hydrophobic faces of the metallacrown, generating a sort of ladder almost aligned with the crystallographic a axis. Two nonequivalent metallacrowns interact directly through their hydrophilic faces by means of five hydrogen bonds. Among these, three are given by the peripheral amino groups, which act as donors toward one ring oxygen, one cavity hydroximato oxygen, and a water molecule coordinated to a copper atom of the adjacent metallacrown. Two additional hydrogen bonds involve the water molecules coordinated to the central Ca^{II}

dx.doi.org/10.1021/ic3013798 | Inorg. Chem. 2012, 51, 11533−11540

which interact with a ring oxygen of the adjacent MC scaffold. On the contrary, the hydrophobic faces of adjacent metallacrown scaffolds do not interact directly, but they rather do through a network of hydrogen bonds, which involve two nitrate ions and three non coordinated water molecules, one water molecule coordinated to Ca^{II} and the methoxide ion. The two nitrate ions also interact in one hydrogen bond with two NH group of indole groups of adjadecent metallacrowns.

The tryptophan residues point away from the scaffold likely as the result of the hydrogen bonds occurring between their NH_{indole} fragments and oxygen atoms from adjacent MC scaffolds, nitrate ions, or cocrystallized water molecules. Surprisingly, despite the large number of aromatic groups, no significant CH-π or $\pi-\pi$ interactions are observed between the indolic groups, which rather prefer to orient in the space in the way to give rise to the described hydrogen bonds. Solvation water and methanol molecules (disordered) are also present in the structure and are involved in a tight net of hydrogen bonds. One single indole group in the structure is not involved in any hydrogen bond through the NH_{indole} fragment because surrounded by other aromatic group, resulting in a marked fluxionality and in large thermal ellipsoids as shown in Figure 1.

Kinetics of Core Ca^{II}–Ln^{III} Substitution. Upon addition of an excess of Ln^{III} nitrates to a solution of Ca(II)[15-$MC_{Cu(II)N(Trpha)}$-5]$^{2+}$ (**1**) in methanol, the expected change of color from brick red to blue-purple connected with the formation of Ln(III)[15-$MC_{Cu(II)N(Trpha)}$-5]$^{3+}$ was observed in few hours, in accordance with the observations reported in the literature for the same systems.[21,24,31] The absorbance maxima progressively changed from 530 nm (Ca(II)[15-$MC_{Cu(II)N(Trpha)}$-5]$^{2+}$) to ca. 575 nm (Ln(III)[15-$MC_{Cu(II)N(Trpha)}$-5]$^{3+}$) as reported in Figure 2a. The spectral set exhibits a clear isosbestic point at ca. 570 nm for all lanthanides except Nd^{III} (Figure 2a and the Supporting Information), which is the result of the very similar absorption maxima of the Ln(III)[15-$MC_{Cu(II)N(Trpha)}$-5]$^{3+}$ species for all lanthanides (see below and ref 24). The differences in the spectral set for Nd^{III} and Er^{III} are accounted for the intrinsic absorption bands of these ions in the visible range. For the same reasons, the isosbestic point in the spectra of Nd^{III}-containing samples do not present the clear isosbestic point as this ion presents an absorption band at *ca.* 565 nm.

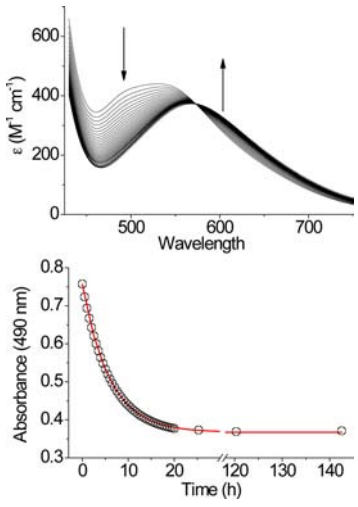

Figure 2. (a) Visible molar absorption spectra of a 1.85 mM solution of **1** in methanolic MES buffer (50 mM, pH 6.2, T = 293 K) added with 10 equiv. of La^{III}. Spectra were recorded every 30 min. (b): Absorbance values at 490 nm as a function of time (same sample as in panel a). The red line represents the absorbance values calculated using the values for the rate constant k reported in Table 2 for La^{III}.

The absorbance values at 490 nm vs time for the reaction of **1** with La^{III} are reported in Figure 2b. For La^{III}, Nd^{III}, and Gd^{III}, the purple color of the final solutions remained unchanged for up to two weeks. On the contrary, for Dy^{III} and Er^{III} the color first changes from brick red to dark purple in *ca.* 20 h, to turn then into green after an additional 5–10 h. This behavior has been already observed for Ln(III)[15-$MC_{Cu(II)N(Pheha)}$-5]$^{3+}$ complexes, and has been connected with the lower stability of the MC with Ln^{III} ions heavier than Er^{III}.[21,24]

To establish the order of the reaction, we calculated the initial rates of the reaction of Ca(II)[15-$MC_{Cu(II)N(Trpha)}$-5]$^{2+}$ with Gd^{III} for different reactant concentrations, using the absorbance at 490 nm of the spectra collected at t = 0, 30, 60, and 90 min after Gd^{III} addition to the MC (**1**) solution. These rates exhibited a linear dependence (first order) in both the initial concentration of reactants **1** and Ln^{III}, and suggests a kinetic law of the second order (see the Supporting Information). The 490 nm wavelength has been chosen as for this wavelength the maximum difference of molar absorbance between tha Ca^{II} and Ln^{III} 15-MC-5 was observed.

The rate constants for the substitution reaction of the core Ca^{II} with Ln^{III} for Ca(II)[15-$MC_{Cu(II)N(Trpha)}$-5]$^{2+}$ were determined under using samples with a 10-fold excess of lanthanide(III) with respect to the metallacrown to accelerate the substitution process. The absorbance spectra were treated using a second-order reaction model, and the rate constants (k) are reported in Table 2. Beause of the color changes observed for heavier lanthanides after 30 h (see above), for all Ln^{III} ions only the spectra collected up to 20 h after the beginning of the reaction were used in the fitting procedures for the calculations of the second order rate constants k, which are reported in Table 2. The absorbance values at 490 nm as a function of time (observed and calculated) are reported as Supporting Information. As reported in Table 2 and Figure 3, the rate constants k decrease from 0.1543 M^{-1} min^{-1} for La^{III} to 0.0720 M^{-1} min^{-1} for Gd^{III}. A small increase from Gd^{III} to Er^{III} was observed (0.106 M^{-1} min^{-1}). At the Ln^{III} and MC concentrations used for the determination of the kinetic constants, (C_{Ln} = 18.5 mM; C_1 = 1.85 mM) the $t_{1/2}$ are on the order of 4–9 h. For the slowest reaction observed for Gd^{III}, 90% of Ca^{II} substitution is obtained in ca. 31 h. Table 2 reports also the second order kinetic constants k_{inv} related to the inverse Ln–Ca substitution, calculated using the stability constants K for the same reaction as $k_{inv} = k/K$. Although the K values were determined in methanol:water 99:1, 50 mM MES buffer and pH 6.5,[24] these conditions are very close to those used here for the determination of the rate constants. The data treatment of the spectral set allowed for the determination of the visible spectral parameters (λ_{max}, ε_{max}) for the Ln(III)[15-$MC_{Cu(II)N(Trpha)}$-5]$^{3+}$ complexes (reported as the Supporting Information), which were highly consistent with those obtained by the thermodynamic studies of the Ca–Ln substitution reaction. Most important, these spectral data prove that the final species obtained in these experiments are the Ln(III)[15-$MC_{Cu(II)N(Trpha)}$-5]$^{3+}$ complexes. A discussion of the trend for the λ_{max} values can be found in refs 3 and 24, taking into account the effect of the larger charge/radius ratio of the central lanthanide on the ligand field of peripheral copper(II) ions.

dx.doi.org/10.1021/ic3013798 | *Inorg. Chem.* 2012, 51, 11533–11540

Table 2. Second-Order Rate Constants (k) for the Ca(II)[15-MC$_{Cu(II)N(Trpha)}$-5]$^{2+}$ + Ln^{3+} → Ln(III)[15-MC$_{Cu(II)N(Trpha)}$-5]$^{3+}$ + Ca^{2+} Reaction in Methanol (MES buffer, pH 6.2, 293 K)[a]

	La^{III}	Nd^{III}	Gd^{III}	Dy^{III}	Er^{III}
ionic radius (Å)	1.216	1.109	1.053	1.027	1.004
k (M^{-1} min^{-1})	0.1543(3)	0.1226(2)	0.0720(6)	0.090(6)	0.106(7)
$t_{1/2}$ (min)[b]	250(1)	314(1)	535(4)	430(30)	360(20)
Log K[c]	4.09(1)	4.05(3)	3.79(3)	3.42(5)	3.07(3)
k_{inv} (× 10^{-5} M^{-1} min^{-1})	1.25(3)	1.09(8)	1.16(8)	3.5(5)	9.1(9)

[a]The table also reports the values of the $t_{1/2}$ (half life) of the Ca(II)[15-MC$_{Cu(II)N(Trpha)}$-5]$^{2+}$ species under the experimental conditions, the thermodynamic constants for the substitution reactions (Log K), and the ionic radii for the different lanthanide ions. The second-order rate constant for the inverse reaction (k_{inv}) calculated from K and k are also reported. [b]The half-life has been calculated using C_{Ln} = 18.5 mM and C_L = 1.85 mM as the initial concentrations. [c]Ref. 24.

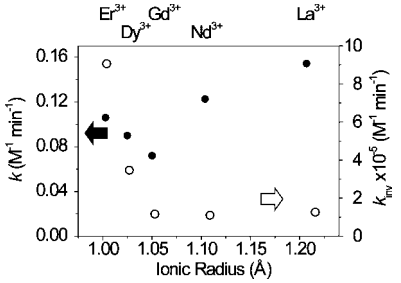

Figure 3. Plot of the values of the second-order rate constants for the Ca(II)[15-MC$_{Cu(II)N(Trpha)}$-5]$^{2+}$ + Ln^{3+} → Ln(III)[15-MC$_{Cu(II)N(Trpha)}$-5]$^{3+}$ + Ca^{2+} reaction in methanol (MES buffer, pH 6.2, 293 K). Forward reaction (k), ●; inverse reaction (k_{inv}), ○.

The slow kinetics of ligand exchange in 15-MC-5 complexes allowed us to investigate if the core metal substitution process occurs by disassembly reassembly of the MC scaffold, or by direct metal substitution. To establish the mechanism, the metallacrowns **1** and **2**, which differ only by the aromatic substituents on the peripheral chelating arm, were dissolved in equimolar amounts in methanol and reacted with 1 equiv. of La^{III}. The brick red solution became purple in a few hours, and it was analyzed after 72 h by ESI-MS. The ESI-MS spectrum before the addition of La^{III} shows two separate multiplets in the region m/z = 1300−1550 (Figure 4a). These signals correspond to the {Ca(II)[15-MC$_{Cu(II)N(L)}$-5](NO$_3$)}$^+$ ions for Pheha (m/z = 1308) and Trpha (m/z = 1504), respectively. Upon addition of La^{III}, two new multiplets appeared in addition to the previous ones (Figure 4b), corresponding to the species {La(III)[15-MC$_{Cu(II)N(Ligand)}$-5](NO$_3$)$_2$}$^+$ (m/z = 1470 for Pheha, 1665 for Trpha). A small signal corresponding to the {La(III)[15-MC$_{Cu(II)N(Trpha)}$-5](NO$_3$)(CH$_3$O)}$^+$ ion has been also observed (m/z = 1634). Most important, the peaks corresponding to the mixed-ligand Ln^{III} metallacrowns were not observed. A control solution was also prepared by mixing lanthanum(III) nitrate, copper(II) acetate and both Trpha and Pheha ligands in equimolar amounts (La:Cu:Pheha:Trpha *ca.* 2:5:6:6). The solution, which was initially green, became purple within few hours, and has been analyzed by ESI-MS 72 h after sample preparation. The spectrum (see the Supporting Information) showed the presence of four signals in the 1200 − 1750 region at m/z = 1509 (30%), 1548 (100%), 1587 (90%), 1626 (25%), corresponding to the mixed metallacrowns {La(III)[15-MC$_{Cu(II)N(Pheha)x(Trpha)y}$-5](NO$_3$)$_2$}$^+$ (x, y = 1−4, x + y = 5).

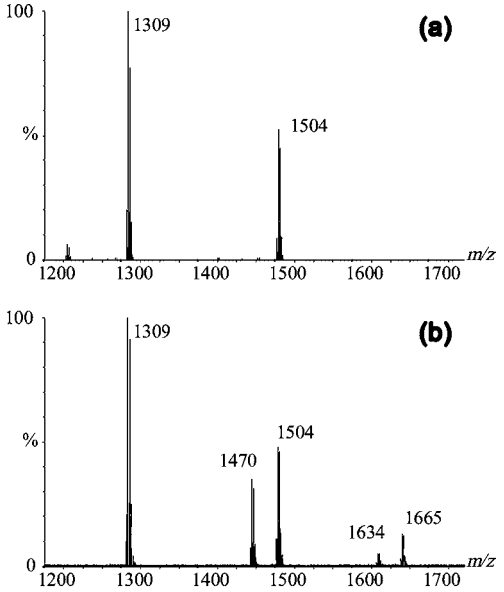

Figure 4. (a) ESI-MS spectra of a solution of **1** and **2** at equimolar concentration in methanol (C_1 = C_2 = 8.9 × 10^{-4} M). (b) ESI-MS spectra of the same solution added with **1** eq. of La^{III} (vs. total MC species) collected 72 h after addition. {Ca(II)[15-MC$_{Cu(II)N(Pheha)}$-5](NO$_3$)}$^+$ m/z = 1309; {La(III)[15-MC$_{Cu(II)N(Pheha)}$-5](NO$_3$)$_2$}$^+$ m/z = 1470); {Ca(II)[15-MC$_{Cu(II)N(Trpha)}$-5](NO$_3$)}$^+$ m/z = 1504; {La(III)[15-MC$_{Cu(II)N(Trpha)}$-5](NO$_3$)(CH$_3$O)}$^+$ m/z = 1634; {La(III)[15-MC$_{Cu(II)N(Trpha)}$-5](NO$_3$)$_2$}$^+$ m/z = 1665.

DISCUSSION

The analysis of the initial rates of reaction for the Ca−Gd substitution indicates that the reaction rate depends on both the lanthanide and metallacrown concentration, and is first order in both of these reactants (see Supporting Information). To determine the second-order kinetic constants, we studied the Ca−Ln substitution using Ln^{III} in 10-fold excess vs. **1** to accelerate the reaction and to observe the significant changes in the visible spectrum within 15−20 h after sample preparation. The kinetic constants reported in Table 2 show that Ca^{II} substitution in the 15-MC-5 complex is fastest with La^{III}, while the slowest rates were observed with Gd^{III}. Actually, the $t_{1/2}$ values are 4−9 h and show that the substitution reaction is faster for lighter lanthanides (La, Nd), reaches a rate minimum for Gd^{III}, and slightly increases again for heavier lanthanides (Dy, Er). The thermodynamics of Ca−Ln substitution in both Ca(II)[15-MC$_{Cu(II)N(Pheha)}$-5]$^{2+}$ and Ca(II)[15-MC$_{Cu(II)N(Trpha)}$-5]$^{2+}$ complexes has been recently examined by spectrophotometry, and these studies allowed us to establish that the

dx.doi.org/10.1021/ic3013798 | Inorg. Chem. 2012, 51, 11533−11540

substitution of core Ca^{II} is spontaneous for all Ln^{III} ions in the La–Yb series, most favored for La^{III} and decreasing along the Ln series. The Ca^{II} substitution by La^{III}, though spontaneous, occurs however within hours along the entire La–Er series. Interestingly, the kinetic constant for the inverse Ln–Ca substitution reaction (k_{inv}) does not change significantly from La^{III} to Gd^{III} (Table 2). This is a consequence of the slight decrease of the kinetic k constant along the La–Gd series, which is compensated by a decrease in the thermodynamic K parameter. On the contrary, in the Gd–Er series the k_{inv} increases as the result of a slight increase of the kinetic k value and a marked decrease of the thermodynamic K parameter (Table 2 and Figure 3). These three parameters (k, k_{inv}, and K) allowed also us to draw an activation energy

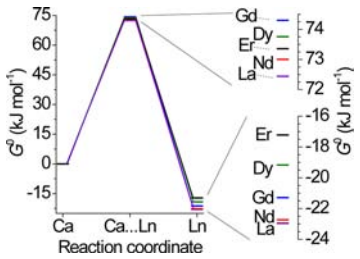

Figure 5. Plot of the free energy for the Ca(II) and Ln(III)[15-$MC_{Cu(II)N(Trpha)}$-5]$^{2+}$ species, and related transition states for the reaction Ca(II)[15-$MC_{Cu(II)N(Trpha)}$-5]$^{2+}$ + Ln^{3+} → Ln(III)[15-$MC_{Cu(II)N(Trpha)}$-5]$^{3+}$ + Ca^{2+} reaction in methanol (MES buffer, pH 6.2, 293 K), calculated from data reported in Table 2.

diagram, which is reported in Figure 5. In this diagram, the free energy change from Ca^{II} to Ln^{III} along the reaction coordinate (ΔG°) has been calculated through the van't Hoff equation using the Ca–Ln substitution K constants reported in the literature.[24] All the parameters used refer to 1 M concentrations as the standard states.

As the 15-MC-5 are self-assembled complexes, the studies presented so far in the literature could not define whether the core metal substitution occurs by a disassembly reassembly pathway of the MC scaffold, or by direct metal substitution.[23−25,44,45] To establish the actual process, and to give an interpretation of the kinetic behavior of the Ca–Ln substitution reaction, we decided to study the possible mechanism of substitution of the core metal through mass spectrometric analyses of the products of the substitution reaction where two Ca^{II} metallacrowns with very similar ligands are involved. This technique proved itself to be a very powerful approach to study both the speciation and the reactivity of self-assembled supramolecular complexes,[46−48] and in the field of metallacrowns it allowed elucidation of the speciation and the integrity of complexes in solution.[15,17,22,49−51] The ESI-MS spectrum of a solution containing both Ca(II)[15-$MC_{Cu(II)N(Trpha)}$-5]$^{2+}$ (**1**) and Ca(II)[15-$MC_{Cu(II)N(Pheha)}$-5]$^{2+}$ (**2**) in methanol showed two separate multiplets related to these two cations. No other peaks are present, ruling out the occurrence of ligand exchange between the two macrocycles in the initial solution. Addition of lanthanum(III) nitrate to the solution resulted in the appearance of two main peaks, in addition to the previous ones, related to the La(III)[15-$MC_{Cu(II)N(Pheha)}$-5]$^{3+}$ and La(III)[15-$MC_{Cu(II)N(Trpha)}$-5]$^{3+}$ species. Mixed-ligands Ln^{III} metallacrowns are, therefore, not obtained starting from preassembled Ca^{II} MC species, but they are the main species when the metallacrowns are assembled from initial components (i.e., mixing Ca^{II}, Cu^{II}, Trpha and Pheha). The absence of peaks corresponding to mixed-ligand metallacrowns as products of the Ca–Ln substitution suggests that this process proceeds through a direct Ca–Ln substitution with no disassembly/reassembly of the metallacrown scaffold. This observation actually accounts for the slow kinetics of the substitution of Ca^{II} by Ln^{III}: although spontaneous, the removal of Ca^{II} from the cavity likely results very demanding in terms of activation energy, as the calcium ion results very well encapsulated in the MC scaffold as observed from the crystal structure of **1**.

The direct core metal substitution for a metallamacrocycle complex at the mechanistic limits may be either dissociative or associative as found, for instance, for the Na^{+} self-exchange reaction in its complex with benzo-15-C-5.[52,53] In the dissociative mechanism, a slow dissociation step of the encapsulated cation leads to an intermediate vacant macrocycle, which then reacts quickly with a free cation to give the product. In contrast, in the associative mechanism (including the interchange associative (I_A) processes) the incoming cation interacts with the metal-macrocycle species, promoting the cation removal from the cavity (e.g., by electrostatic repulsion) with formation of the product. In particular, it has been found that the conformational flexibility of the macrocycle controls the rate of the associative mechanism, while the solvation effects on the leaving cation control the rate of the dissociative mechanism.[52−54] The kinetic law for the Ca–Ln substitution reaction for Ca(II)[15-$MC_{Cu(II)N(Trpha)}$-5]$^{2+}$ is second order overall and this likely rules out the occurrence of a dissociative mechanism (which should be first order in **1**) in favor of an associative process. A dissociative pathway would in fact go through the formation of an intermediate vacant 15-MC-5 containing five negative oxygen atoms in the cavity that are not bound to a core metal. This species, although found for Ni^{II},[50] has never been observed with Cu^{II} and it is likely a high-energy species for this metal.[3,15] The dissociative mechanism results, therefore, in a high activation energy, which makes the associative (or interchange associative) pathway preferred over a dissociative substitution. Finally, the quite slow reaction rates for the Ca–Ln substitution reaction find an explanation in the favorable Ca^{II} encapsulation as suggested above, and in the rigidity of the 15-MC-5 scaffold, which possesses a limited conformational flexibility.

Although the present data eliminate only the dissociative mechanism and do not fully describe the nature of the interactions between the cations and the MC scaffold along the reaction coordinate, the structural and thermodynamic data available in the literature on these complexes allows us to account for the trends in the kinetic parameters reported in Table 2 and Figure 3. The crystal structures of La^{III} and Nd^{III} 15-MC-5 reported in the literature showed that these two large core metals are not completely encapsulated in the cavity, as for them the interaction with the oxygens of the cavity is optimal when the ions are slightly off the mean oxygens plane.[2,21,29] This structural feature explains the faster Ca^{II} substitution observed for larger lanthanides. In the transition state these ions likely interact side-on with the metallacrown cavity, and this in turn results in a lower activation energy and a faster reaction. On the other hand, the smaller dimensions of Dy^{III} and Er^{III} compared to Gd^{III} account for a slightly faster Ca–Ln substitution as the result of their higher charge density. While approaching the MC scaffold, the smaller Ln^{III} ions interact more favorably than the lighter lanthanides with the negatively

charged region of the MC scaffold (i.e., the oxygen atoms in the cavity) resulting in faster rate constants compared to that of Gd^{III}.

As regards the inverse reaction, La^{III}, Nd^{III}, and Gd^{III} possess similar low k_{inv} rate constants. In contrast, the smaller lanthanides (Dy^{III}, Er^{III}) possess remarkably higher k_{inv}. We believe that the faster removal of Dy^{III} and Er^{III} by Ca^{II} is related to the smaller dimension of the heavier lanthanides, which interact relatively weakly with the oxygens of the cavity (lower stability as encapsulated ions), resulting in a lower energy demand for their displacement and a higher reaction rate.

CONCLUSION

In this paper, we presented a kinetic and mechanistic study of the reaction of core Ca^{II} substitution by lanthanide(III) ions in methanolic solution. The results were compared to the thermodynamic parameters for the same reaction. Lighter lanthanides show a kinetic rate which significantly decreases along the lanthanide series to Gd^{III}, whereas a small increase is observed for heavier lanthanides. On the basis of the thermodynamic log K for the same reaction the inverse Ln−Ca substitution reaction could be also calculated, showing that the displacement of lanthanides by Ca^{II} is faster for heavier ions, while no differences are observed for Gd^{III} and the lighter lanthanides. These kinetic and thermodynamic effects were interpreted on the basis of the capability of the core metal ions to interact with the cavity.

The main conclusions of these studies can be summarized as follows: (1) While a thermodynamic selectivity for the Ca−Ln substitution (i.e., marked differences in K values) was observed for heavier lanthanides, quite the opposite is found for the kinetic parameters. In terms of reaction rates, in fact, the largest differences were observed for the lighter lanthanides, demonstrating a slight kinetic selectivity for these ions. 2) A marked kinetic selectivity is observed for the inverse Ln−Ca substitution reaction with heavier lanthanides, while no differences are observed for lighter ones. (3) The optimal interaction of the core ions with the five oxygens of the cavity is the basis of the observed trends for the reaction rates, as the energies connected with this interaction sums up to the cation desolvation energies. Because Ca^{II} is well encapsulated in the MC cavity, the highest Ca−Ln substitution rates were observed for the larger lathanides which do not required complete encapsulation. On the other hand, the inverse Ln−Ca substitution process are faster when the optimal Ln−oxygen interaction is lost, as observed for smaller, heavier lanthanides ions (Dy^{III}, Er^{III}).

ASSOCIATED CONTENT

Supporting Information

X-ray crystallographic information of the X-ray structure in CIF format (CCDC 888604). Additional figures of structural details, experimental visible spectra, results of data treatment. This material is available free of charge via the Internet at http://pubs.acs.org.

AUTHOR INFORMATION

Corresponding Author

*E-mail: vlpec@umich.edu.

Notes

The authors declare no competing financial interest.

ACKNOWLEDGMENTS

V.L.P. thanks the National Science Foundation for financial support (CHE 0111428 and CHE 1057331). M.T. thanks the Italian Ministery of Foreign Affairs (Direzione Generale per la Promozione del Sistema Paese) for the Significant bilateral project, S&T Italy-USA 2011-12. The C.I.R.C.M.S.B. (Consorzio Interuniversitario di Ricerca in Metalli nei Sistemi Biologici (Bari, Italy)) and the European Group of Thermodynamics of Metal Complexes are also acknowledged.

REFERENCES

(1) Pecoraro, V. L.; Stemmler, A. J.; Gibney, B. R.; Bodwin, J. J.; Wang, H.; Kampf, J. W.; Barwinski, A. *Prog. Inorg. Chem.* **1997**, *45*, 83−177.
(2) Mezei, G.; Zaleski, C. M.; Pecoraro, V. L. *Chem. Rev.* **2007**, *107*, 4933−5003.
(3) Tegoni, M.; Remelli, M. *Coord. Chem. Rev.* **2012**, *256*, 289−315.
(4) Lah, M. S.; Pecoraro, V. L. *J. Am. Chem. Soc.* **1989**, *111*, 7258−7259.
(5) Pecoraro, V. L. *Inorg. Chim. Acta* **1989**, *155*, 171−173.
(6) Gibney, B. R.; Wang, H.; Kampf, J. W.; Pecoraro, V. L. *Inorg. Chem.* **1996**, *35*, 6184−6193.
(7) Lah, M. S.; Pecoraro, V. L. *Inorg. Chem.* **1991**, *30*, 878−880.
(8) Kessissoglou, D. P.; Bodwin, J. J.; Kampf, J.; Dendrinou-Samara, C.; Pecoraro, V. L. *Inorg. Chim. Acta* **2002**, *331*, 73−80.
(9) Lah, M. S.; Gibney, B. R.; Tierney, D. L.; Penner-Hahn, J. E.; Pecoraro, V. L. *J. Am. Chem. Soc.* **1993**, *115*, 5857−5858.
(10) Gibney, B. R.; Kessissoglou, D. P.; Kampf, J. W.; Pecoraro, V. L. *Inorg. Chem.* **1994**, *33*, 4840−4849.
(11) Kurzak, B.; Farkas, E.; Glowiak, T.; Kozlowski, H. *J. Chem. Soc., Dalton Trans.* **1991**, 163−167.
(12) Halfen, J. A.; Bodwin, J. J.; Pecoraro, V. L. *Inorg. Chem.* **1998**, *37*, 5416−5417.
(13) Bodwin, J. J.; Pecoraro, V. L. *Inorg. Chem.* **2000**, *39*, 3434−3435.
(14) Tegoni, M.; Ferretti, L.; Sansone, F.; Remelli, M.; Bertolasi, V.; Dallavalle, F. *Chem.—Eur. J.* **2007**, *13*, 1300−1308.
(15) Careri, M.; Dallavalle, F.; Tegoni, M.; Zagnoni, I. *J. Inorg. Biochem.* **2003**, *93*, 174−180.
(16) Tegoni, M.; Dallavalle, F.; Belosi, B.; Remelli, M. *Dalton Trans.* **2004**, 1329−1333.
(17) Tegoni, M.; Remelli, M.; Bacco, D.; Marchiò, L.; Dallavalle, F. *Dalton Trans.* **2008**, 2693−2701.
(18) Psomas, G.; Dendrinou-Samara, C.; Alexiou, M.; Tsohos, A.; Raptopoulou, C. P.; Terzis, A.; Kessissoglou, D. P. *Inorg. Chem.* **1998**, *37*, 6556−6557.
(19) Psomas, G.; Stemmler, A. J.; Dendrinou-Samara, C.; Bodwin, J. J.; Schneider, M.; Alexiou, M.; Kampf, J. W.; Kessissoglou, D. P.; Pecoraro, V. L. *Inorg. Chem.* **2001**, *40*, 1562−1570.
(20) Kessissoglou, D. P.; Kampf, J.; Pecoraro, V. L. *Polyhedron* **1994**, *13*, 1379−1391.
(21) Zaleski, C. M.; Cutland-VanNoord, A. D.; Kampf, J. W.; Pecoraro, V. L. *Cryst. Growth Des.* **2007**, *7*, 1098−1105.
(22) Mezei, G.; Kampf, J. W.; Pan, S.; Poeppelmeier, K. R.; Watkins, B.; Pecoraro, V. L. *Chem. Commun.* **2007**, 1148−1150.
(23) Seda, S. H.; Janczak, J.; Lisowski, J. *Eur. J. Inorg. Chem.* **2007**, 3015−3022.
(24) Tegoni, M.; Furlotti, M.; Tropiano, M.; Lim, C. S.; Pecoraro, V. L. *Inorg. Chem.* **2010**, *49*, 5190−5201.
(25) Stemmler, A. J.; Barwinski, A.; Baldwin, M. J.; Young, V.; Pecoraro, V. L. *J. Am. Chem. Soc.* **1996**, *118*, 11962−11963.
(26) Bodwin, J. J.; Cutland, A. D.; Malkani, R. G.; Pecoraro, V. L. *Coord. Chem. Rev.* **2001**, *216−217*, 489−512.
(27) Jankolovits, J.; Lim, C.-S.; Mezei, G.; Kampf, J. W.; Pecoraro, V. L. *Inorg. Chem.* **2012**, *51*, 4527−38.
(28) Grant, J. T.; Jankolovits, J.; Pecoraro, V. L. *Inorg. Chem.* **2012**, *51*, 8034−8041.

(29) Zaleski, C. M.; Lim, C. S.; Cutland-Van, N.; Kampf, J. W.; Pecoraro, V. L. *Inorg. Chem.* **2011**, *50*, 7707−7717.
(30) Cutland, A. D.; Malkani, R. G.; Kampf, J. W.; Pecoraro, V. L. *Angew. Chem., Int. Ed. Engl.* **2000**, *39*, 2689−2691.
(31) Pacco, A.; Parac-Vogt, T. N.; van Besien, E.; Pierloot, K.; Gorller-Walrand, C.; Binnemans, K. *Eur. J. Inorg. Chem.* **2005**, 3303−3310.
(32) Seda, S. H.; Janczak, J.; Lisowski, J. *Inorg. Chim. Acta* **2006**, *359*, 1055−1063.
(33) *IBM SPSS Statistics v. 20.0.0*; IBM Corporation: Armonk, NY, 2011.
(34) Binstead, R. A.; Zuberbühler, A. D.; Jung, B. *SPECFIT/32*, Bio-Logic SAS, Claix, France, 2004.
(35) Sheldrick, G. M. *CELL_NOW - Program for Indexing Twins and Other Problem Crystals, v. 2008/2*; University of Göttingen: Göttingen, Germany, 2008.
(36) Sheldrick, G. M. *Saint Plus, v. 7.34*; Bruker Analytical X-ray: Madison, WI, 2006.
(37) Sheldrick, G. M. *TWINABS - Program for Empirical Absorption Correction of Area Detector Data, v. 2008/1*; University of Göttingen: Göttingen, Germany, 2008.
(38) Sheldrick, G. M. *SHELXTL, v. 2008/3*; Bruker Analytical X-ray, Madison, WI, 2008.
(39) Cutland, A. D.; Halfen, J. A.; Kampf, J. W.; Pecoraro, V. L. *J. Am. Chem. Soc.* **2001**, *123*, 6211−6212.
(40) Shannon, R. *Acta Crystallogr., Sect. A* **1976**, *32*, 751−767.
(41) Zaleski, C. M.; Depperman, E. C.; Kampf, J. W.; Kirk, M. L.; Pecoraro, V. L. *Inorg. Chem.* **2006**, *45*, 10022−10024.
(42) Cutland-Van Noord, A. D.; Kampf, J. W.; Pecoraro, V. L. *Angew. Chem., Int. Ed.* **2002**, *41*, 4667−4670.
(43) Tegoni, M.; Tropiano, M.; Marchiò, L. *Dalton Trans.* **2009**, 6705−6708.
(44) Stemmler, A. J.; Kampf, J. W.; Pecoraro, V. L. *Angew. Chem., Int. Ed.* **1996**, *35*, 2841−2843.
(45) Parac-Vogt, T. N.; Pacco, A.; Goerller-Walrand, C.; Binnemans, K. *J. Inorg. Biochem.* **2005**, *99*, 497−504.
(46) Charbonnière, L. J.; Gilet, M.-F.; Bernauer, K.; Williams, A. F. *Chem. Commun.* **1996**, 39−40.
(47) Charbonnière, L. J.; Williams, A. F.; Frey, U.; Merbach, A. E.; Kamalaprija, P.; Schaad, O. *J. Am. Chem. Soc.* **1997**, *119*, 2488−2496.
(48) Provent, C.; Rivara-Minten, E.; Hewage, S.; Brunner, G.; Williams, A. F. *Chem.—Eur. J.* **1999**, *5*, 3487−3494.
(49) Dallavalle, F.; Tegoni, M. *Polyhedron* **2001**, *20*, 2697−2704.
(50) Bacco, D.; Bertolasi, V.; Dallavalle, F.; Galliera, L.; Marchetti, N.; Marchio, L.; Remelli, M.; Tegoni, M. *Dalton Trans.* **2011**, *40*, 2491−2501.
(51) Jankolovits, J.; Andolina, C. M.; Kampf, J. W.; Raymond, K. N.; Pecoraro, V. L. *Angew. Chem., Int. Ed.* **2011**, *50*, 9660−9664.
(52) Brière, K. M.; Detellier, C. *Can. J. Chem.* **1992**, *70*, 2536−2543.
(53) Brière, K. M.; Detellier, C. *J. Phys. Chem.* **1992**, *96*, 2185−2189.
(54) Izatt, R. M.; Pawlak, K.; Bradshaw, J. S.; Bruening, R. L. *Chem. Rev.* **1995**, *95*, 2529−2586.